Optimization of multiple robot configuration pattern using shape variant approach

N.S. Osman, M.A.A. Rahman*, A.A.A. Rahman, S.H. Kamsani, and B.M.B. Mohamad

Integrated Manufacturing System (I'Ms), Advanced Manufacturing Centre (AMC), Faculty of Manufacturing Engineering, Universiti Teknikal Malaysia Melaka, Hang Tuah Jaya, 76100 Melaka, Malaysia

*Corresponding e-mail: arfauz@utem.edu.my

Keywords: Industrial robot; multiple robot configuration; variant-shaped approach

ABSTRACT – This work presents a fundamental approach for easily configuring multiple robot within work cell. The works aim to provide fast configuration proposal with less human involvement at low or no further investment. A mathematical model has been developed based on the variant-shaped of robot layout used within manufacturing industry. The model is capable to provide the possible number of configuration, N_c for different number of robot, N_r. The current outcome is to be used for further investigation in providing the optimum layout, L_{opt} for configuring multiple robot work cell.

1. INTRODUCTION

Configuring multiple robot is a challenging work that requires high investment [1], long commissioning time and numbers of human experts [2–4]. This raises issue to simplify current configuration techniques in order to deal with variation of production needs and manufacturing strategy. The initial study by Rahman [5] as shown in Figure 1 on a two dimensional robot work cell with its safety clearance in the form of square shape will be utilized.

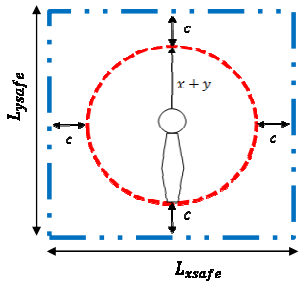

Figure 1 Illustration of two dimensional robot work cell with safety clearance [5]

The Equation 1 is the key to the formulation of variant-shaped of robot work cell and configuration pattern. It will help user to determine the overall safe working area, A_{safe} of the desired layout during the installation.

$$A_{safe} = L_{xsafe} \times L_{ysafe} = 2(X+Y+C) \times 2(X+Y+C) \quad (1)$$

Where,
X: Length of robot arm (mm)
Y: Length of the robot tooling and work piece (mm)
C: Clearance for the worker movement in a work cell (mm)

2. METHODOLOGY

The development process is divided into 2 stages as shown in Figure 2.

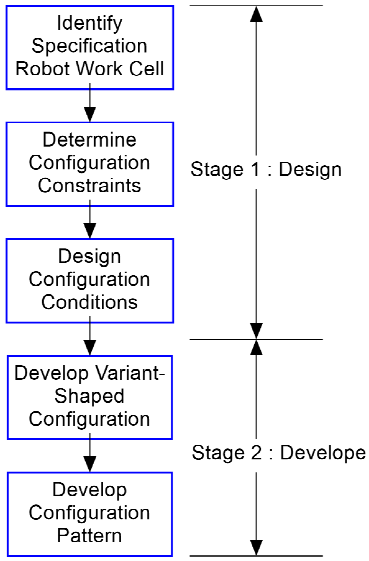

Figure 2 General development process

The first stage focuses on the design aspects which include the robot specifications as well as the configuration constraints and conditions. The specifications of robot work cell were taken as reference based on Rahman works [5]. The constraints involved exclude the corner, half facing, diagonal and mix arrangement. The conditions were selected without considering rigid transformation condition (translation, rotation, reflection or glide reflection). The later stage involves the development of the variant shaped configuration and its pattern. The variant shaped is formed by joining one or more equal squares side by side according to the quantity of robot used. The configuration pattern was developed using the represented possible configuration data with the respective number of robots used as shown in Table 1.

Table 1 Variant-shaped configuration layout data

Number of Robot Used, N_r	1	2	3	4	5	6	7	8	9	10
Number of Configuration, $N_{c,initial}$	1	1	2	5	12	35	108	369	1285	4655

Next, the developed configuration pattern will be optimized.

3. RESULTS AND DISCUSSION

Based on the configuration results in Table 1, the

following configuration pattern and its residuals were successfully developed using MATLAB as shown in Figure 3 and 4 respectively. 9th polynomial with center and scale data checkbox was used to improve the precision of the developed pattern.

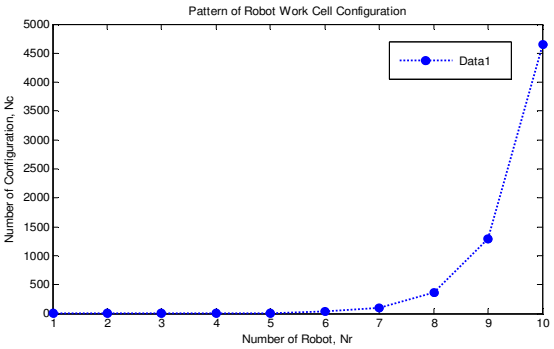

Figure 3 Configuration pattern

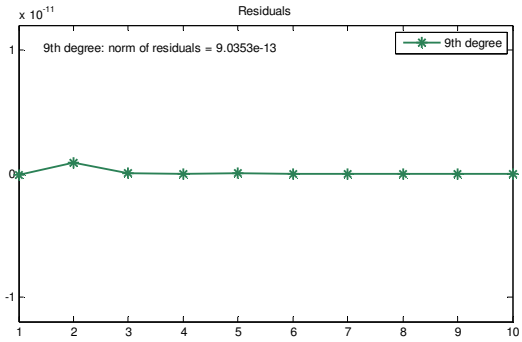

Figure 4 Residuals of configuration pattern

$$N_{c,initial} = 32.754z^9 + 49.733z^8 - 41.258z^7 - 2.469e^{-12}z^6 + 189.69z^5 + 184.84z^4 + 107.78z^3 + 100.01z^2 + 66.556z + 20.635 \quad (2)$$

Where;
$z = (N_r - 5.5) / 3.0277$ is the centered and scaled

Equation 2 was extracted through curve fitting of 9th polynomial and it is able to determine the number of configuration. During the stage, norm residual was used to determine the difference between an ordinate data value and a corresponding fit value at a specific abscissa value. Norm of residuals for the configuration pattern is $9.0353e^{-13}$. The developed configuration pattern was later optimized by grouping the number of configuration into the columns configuration. It was grouped according to the same total number of robot in the references line at the horizontal plane. As a results, a number of columns configuration, $N_{c,c}$ and its pattern can be tabulated as shown in Table 2 and Figure 5 respectively.

Table 2 Columns configuration layout data

Number of Robot Used, N_r	1	2	3	4	5	6	7	8	9	10
Number of Columns Configuration, $N_{c,c}$	1	2	3	4	5	6	7	8	9	10

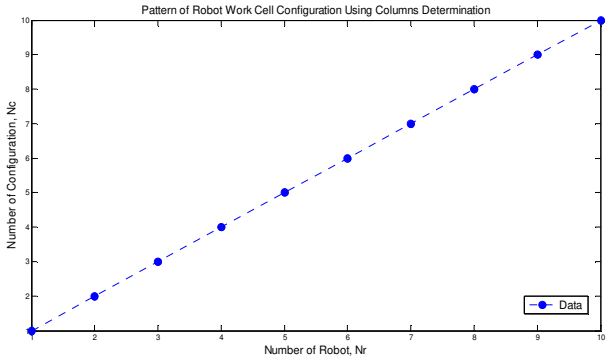

Figure 5 New configuration pattern

Later, a new linear relationship can be extracted as in Equation 3.

$$N_{c,c} = N_r \quad (3)$$

At this stage, the configuration pattern and equation have been optimized and the complexity have been reduced.

4. CONCLUSIONS

The current work for configuring multiple robots was based on the variant-shaped layout. The configuration pattern and its equation were successfully developed and extracted. The mathematical model was optimized using MATLAB and successfully met the desired outcome. The next stage will focus on using computational capability towards determining the optimum robot work cell, L_{opt}.

REFERENCES

[1] R. Kia, F. Khaksar-Haghani, N. Javadian, and R. Tavakkoli-Moghaddam, "Solving a multi-floor layout design model of a dynamic cellular manufacturing system by an efficient genetic algorithm," *J. Manuf. Syst.*, vol.33, no. 1, pp. 218–232, 2014.

[2] M. A. A. Rahman, "*Executable Framework for Reconfigurable Flexible Manufacturing System*," RMIT University, 2014.

[3] D. Spensieri, J. S. Carlson, R. Bohlin, J. Kressin, and J. Shi, "Optimal Robot Placement for Tasks Execution," *Procedia CIRP*, vol. 44, pp. 395–400, 2016.

[4] M. A. A. Rahman, N. S. Osman, C. H. Boon, G. L. T. Poh, A. A. A. Rahman, B. M. B. Mohamad, S. H. Kamsani, E. Mohamad, Z. A. Zaini, and M. F. A. Rahman, "Configuring Safe Industrial Robot Work Cell in Manufacturing Industry," *J. Adv. Manuf. Technol.*, vol. 10, no. 2, 2016.

[5] M. A. A. Rahman, "Improvement of Safety System Installation for Industrial Robot Work Cell," Universiti Tenaga Nasional, 2005.

Proceedings of Innovative Research and Industrial Dialogue'16, pp. 3-4 (May 2017)

Development of an underactuated robotic hand for industrial work

M.A.M.Yuden[1], M.M. Ghazaly[1,*], A.C. Amran[2], I.W. Jamaludin[1]

[1)] Centre for Robotics and Industrial Automation (CeRIA), Faculty of Electrical Engineering, Universiti Teknikal Malaysia Melaka, Hang Tuah Jaya, 76100 Durian Tunggal, Melaka, Malaysia

[2)] Faculty of Engineering and Technology, Universiti Teknikal Malaysia Melaka, Hang Tuah Jaya, 76100 Durian Tunggal, Melaka, Malaysia

[*]Corresponding e-mail: mariam@utem.edu.my

Keywords: Underactuated robotic hand; finite element analysis (FEA); open-loop characteristics

ABSTRACT – Industrial sector exposes workers to high safety risks. These risks can be reduced by designing robotic hand that is able to replace human works. Therefore, this study proposes a development of an underactuated dexterous robotic hand for industrial work. The design must be considered robustness, low cost and has minimum Degree of Freedom (DOF) but can achieve dexterous grasp. To achieve this, a 3D printed underactuated robotic hand is designed and fabricated. The aim of this study is to investigate the robustness of robotic hand by Finite Element Analysis (FEA) and to characterize the open-loop characteristic of robotic finger.

1. INTRODUCTION

Robotic hand plays an important role in the industrial sector application to handle the works that are unreachable or dangerous to human. A dexterous robotic hand is defined as a robotic hand which is skilful since each joint is separately actuated in order to drive all fingers. Nowadays, many researchers developed various types of robotic hands according to their application. The selection of actuator, material, number of finger, joint and DOF must be considered in designing robotic hand. Underactuated robotic hands and actuated robotic hands have been developed for the past few years. Every design has its own advantages and disadvantages. Advantage of the underactuated robotic hand is simple and low cost to manufacture [1]. Underactuated robotic hand is applied to reduce the number of actuator, weight and cost of the robotic hand but can dexterously grasp object with minimum number of components [2]. Meanwhile, the design of actuated robotic hand is more complex and highly cost but it can be controlled precisely and more robust [3]. Moreover, the implementation of actuator directly to the system design produced high precision and high speed response [4]. Recently, 3D printing technologies are widely used in the development of the robotic hands. The simplicity and low cost of operation [1] cause 3D printing to get high demand in producing the prototype.

Therefore, this paper focuses on the development of an underactuated robotic hand design for industrial works include study the robustness and characterize the open-loop characteristic of the robotic finger. The design must be considered the robustness, low cost and has minimum DOF but can dexterously grasp object.

2. METHODOLOGY

2.1 Parameter Design of the Robotic Hand

The material used for the robotic hand is Acrylonitrile Butadiene Styrene (ABS) plastic and is printed by using 3D printer. The robotic hand design has three fingers and a thumb. Each finger and thumb has two links and 2DOF. Each joint of the finger is actuated by Faulhaber DC Micro Motor Series 1024SR combined with planetary gearheads series 12/4 with reduction ration 256:1. The transmission mechanism between motor and joint is using a set of bevel gear. Each motor has an optical encoder to measure the position and angular rotation of the finger flexion. The size and structure of the robotic hand is designed to be as human-like hand and Table 1 shows the parameters design for fabricating the robotic hand while Figure 1 shows the experimental setup of the underactuated robotic hand system.

Table 1 Parameter design of robotic hand

Parameter	Size (LxWxH)	Mass
Fingertip	25x18x61 mm	0.0110 kg
Finger link	25x18x72 mm	0.0150 kg
Thumb link	25x25x67 mm	0.0490 kg
Palm	100x20x124 mm	0.0520 kg
DC micro motor with encoder	13x13x63 mm	0.0318 kg
	Total Mass	0.4444 kg

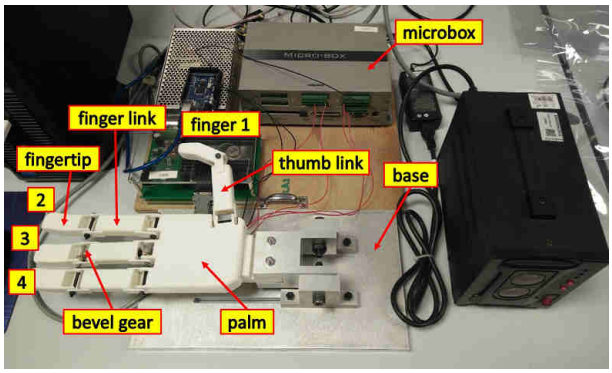

Figure 1 Developed of robotic hand experimental setup

2.2 Finite Element Analysis

The robustness of the robotic hand was studied by using FEA via Solidworks software. The load amount of force is set at each of selected part of robotic hand which

is at the fingertips and palm. The application of this force represents the robotic hand during grasping and picking up the object. The force is varied from 0 N to 12.5 N at every fingertip, so the total maximum force exerted on the robotic hand is 50N. The maximum stress at the part of robotic hand is observed and analyzed.

2.3 Open-Loop Characteristic of Robotic Finger

System identification tool is used to obtain the transfer function of the motor that move the Fingertip 3 by using Simulink block diagram. The transfer function obtained is recorded and compared with the transfer function derived from free body diagram. Figure 2 shows the system modeling of Fingertip 3. The transfer function for the robotic hand is shown by Equation 1.

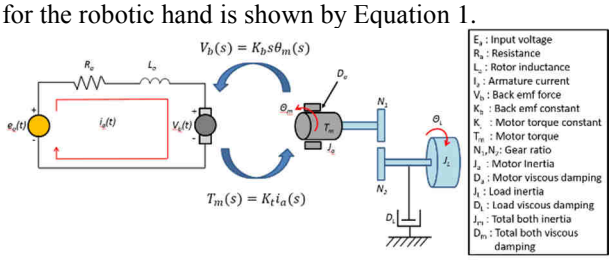

Figure 2 Free body diagram fingertip 3

$$\frac{\theta_L(s)}{E_a(s)} = \frac{K_t/R_a}{J_m s^2 + \left(D_m + \frac{K_t K_b}{R_a}\right)s} \bullet \frac{N_1}{N_2} \qquad (1)$$

3. RESULTS AND DISCUSSION

3.1 Finite Element Analysis

Figure 3 shows the equivalent stress results of ABS printed robotic hand due to the applied force. From the result, it can be observed that the joints of the fingers area and fingers holder have critical Von-Mises stress which is around $1.8\text{x}10^6$ N/m^2 to $3.6\text{x}10^6$ N/m^2. It shows that the maximum Von-Mises stress is still below the tensile strength of itself which is $3.7\text{x}10^7$ N/m^2 for ABS plastic. Based on the FEA, the structure is safe to grasp and pick up an object with the force equivalent to 50 N.

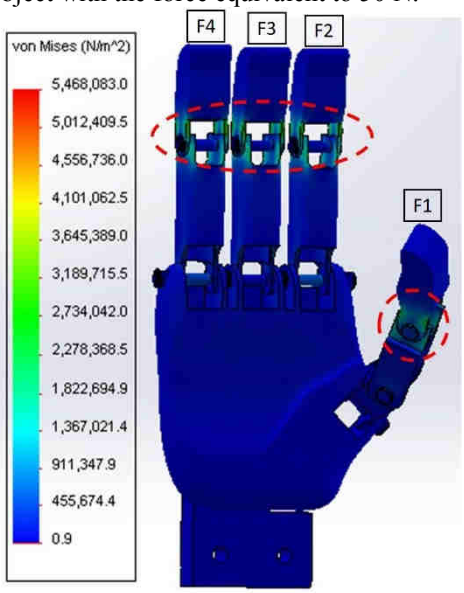

Figure 3 Equivalent stress due to the force applied

3.2 Open-Loop Characteristic of Robotic Finger

Figure 4 shows the comparison between the transfer function obtained from system identification tool and derived from the free body diagram. From the graph, both errors of transfer functions are stable and consistent along the period of the system at which maximum error of transfer function obtained from system identification tool is 0.43° and 0.57° for free body diagram when step input signal is 1.0 s to 2.0 s.

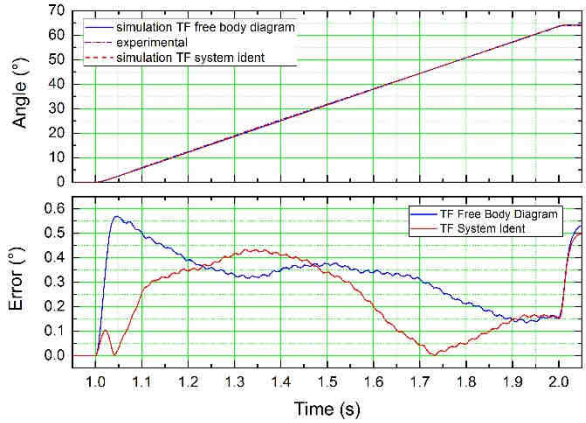

Figure 4 Comparison of transfer functions

4. CONCLUSIONS

In conclusion, the developed robotic hand is strong enough to grasp object, low cost and has minimum DOF. By FEA, the maximum Von-Mises stress for the robotic hand is around $1.8\text{x}10^6$ N/m^2 to $3.6\text{x}10^6$ N/m^2 and safe for the structure to grasp object. The open-loop experiment shows the maximum error between simulation and experimental for both transfer functions are 0.43° and 0.57° respectively. For future works, a suitable controller will be designed for the underactuated robotic hand system.

ACKNOWLEDGEMENT

Authors are grateful to Universiti Teknikal Malaysia Melaka for supporting the research. This research and its publication are supported by Research Acculturation Collaboration Effort (RACE) grant no. RACE/F3/TK5/FKE/F00249 and the Fundamental Research Grant Scheme (FRGS) no.FRGS/1/2016/TK04/FKE-CERIA/F00305.

REFERENCES

[1] V. Kumar and E. Todorov, "A low-cost and modular, 20-DOF anthropomorphic robotic hand: design, actuation and modeling," *13th IEEE-RAS Int. Conf. Humanoid Robot 2013*, pp. 368–375.

[2] Z. Jingdong, L. Jiang, S. Shi, H. Cai, G. Hirzinger "A five-fingered underactuated prosthetic hand system," *IEEE Int. Conf. Mechatronics Autom. ICMA 2006*, pp. 1453–1458.

[3] T. Endo et al. "Five-fingered haptic interface robot: HIRO III," *IEEE Trans. Haptics*, vol. 4, no. 1, pp. 14–27, 2011.

[4] M.M. Ghazaly et al., "Point-To-Point (PTP) Control Performances of an Upper Limb Robotic Arm", *Jurnal Teknologi*, vol. 78, no. 7, pp. 131-140, 2016.

Proceedings of Innovative Research and Industrial Dialogue'16, pp. 5-6 (May 2017)

Effect of ultrasonic and vacuum system assisted mid-end fused deposition modeling to improve printed parts surface finish

A.S. Mohamed[1], S. Maidin[1,*], J.H.U. Wong[1], N.M. Arif[1], W.F.A. Romlee[1] , S.B. Mohamed[2]

[1)]Faculty of Manufacturing Engineering, Universiti Teknikal Malaysia Melaka, Hang Tuah Jaya, 76100 Durian Tunggal, Melaka, Malaysia

[2)]Research Management, Innovation, and Commercialization Centre, Universiti Sultan Zainal Abidin, Gong Badak Campus, 21300, Kuala Terengganu, Terengganu, Malaysia

[*]Corresponding e-mail: shajahan@utem.edu.my

Keywords: Fused deposition modeling; ultrasonic; vacuum system

ABSTRACT - Fused Deposition Modeling (FDM) is a 3D printing technology uses thermoplastic filament. However, despite of fully functional prototypes and geometric complexity, the surface quality of parts produced is undesirable. The aim of this paper is to investigate the effect of applying ultrasonic frequency and vacuum system pressure for improving the printed surface quality of FDM. A transducer firmly attached onto the printer platform and the 3D printer remains in a vacuum chamber. The results showed 14 % (16.2 µm) of ultrasonic assisted and 9 % (17.3 µm) of vacuum assisted system improved surface finish compared to normal printing.

1. INTRODUCTION

Fused Deposition Modelling (FDM) developed by Stratasys Inc., has become one of the most used technique to create a 3D object rapid prototyping. In this process, the part is built as layer upon layer deposition of a spool material. The extruder will extrude the semi molten material into thin layers and deposited by a heated nozzle onto a fixtureless platform. [1-2]. Despite of its tremendous offering this technology present the limitation related to surface finish quality of part printed. The common problem of staircase effect markedly affects FDM parts as it employs thick filament. These problems limit the part surface finishing which is an important requirement to assure component functionality [2-3]. Conversely ultrasound is a sound that frequencies that is greater than 20 kHz. Ultrasound is a proven technology that has been extensively used for machining and it has been claimed to improve surface quality for work piece [4]. Vacuum technology has been applied in various areas of studies and applications due to its unique capability to change the environment by decreasing the atmospheric pressure to suit the specific condition of the research. Vacuum will prevent or reduce the convection process from occurring and heat loss from the source can be maintained in longer period of time depending on vacuum range. Thus, no thermal energy will be able to transmit easily by convection across the vacuum environment [56]. The aim of this paper is to introduce an idea of applying two principals; ultrasonic and vacuum system in order to improve the surface finish quality of FDM parts printed.

2. METHODOLOGY AND EXPERIMENTAL SETUP

This experiment conducted in two different ways, Figure 1 and 2 shows the experimental setup for both principals, ultrasonic-assisted and vacuum-system-assisted UP Plus 2 FDM 3D. The material used for this experiment is ABS thermoplastic. Deposition parameters for this experiment, layer thickness and fill of density are set with default setup as influence factor that would affect the surface finish quality.

Figure 1 Ultrasonic assisted

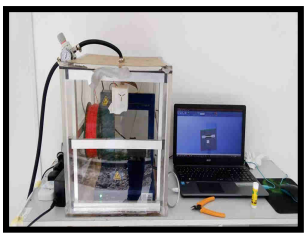

Figure 2 Vacuum system assisted

To aid the ultrasonic-assisted experiment, a common piezoelectric transducer performing in a horizontal wave mode fixedly attached in contact onto the platform of FDM machine. A function generator with a maximum power of 20V comes with alterable frequency used to supply electrical power to generate a desirable frequency. The ultrasonic energy supply only focusing on 20kHz. To run vacuum-system-assisted experiment an acrylic 12mm thickness and inner dimension 350x390mx400mm rectangular shape size securely closed, remain inside with UP Plus 2 printer. Connected with oil-flooded-vacuum-pump to absorb atmospheric air to create a vacuum pressure of 19inHg. Figure 3 shows surface roughness test used a portable surface roughness tester Mitutoyo SJ-301. The method of data construction is Ra technique. To conform the reliability of the result, another approach performed which using optical microscope as shown in Figure 4.

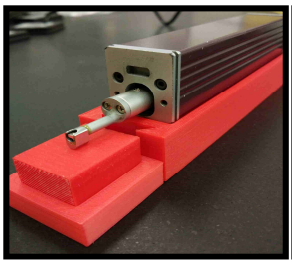

Figure 3 Surface roughness test

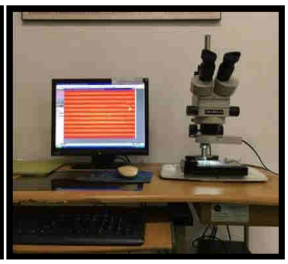

Figure 4 Optical microscope

3. RESULT AND DISCUSSION

The experiment result focusing on the most regular and fine lines produced. Figure 5 shows the bar chart comparison of surface roughness value between non-assisted and assisted FDM printed part. From the result, it shows there is an improvement by using ultrasonic and vacuum system assisted. Based on the graph there are significantly reduction surface finish value compared between non-assisted and assisted. The improvement of Ultrasonic assisted reducing almost 14%, while vacuum system assisted 9% of the surface roughness value.

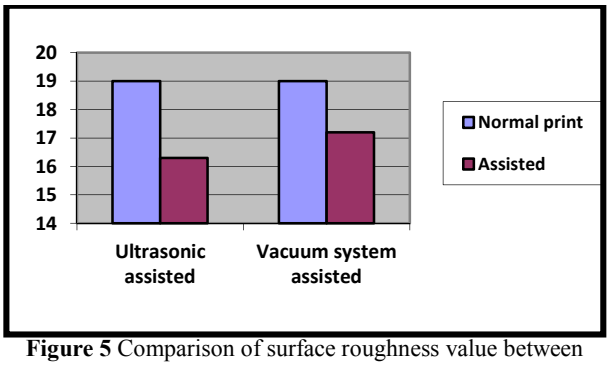

Figure 5 Comparison of surface roughness value between normal and assisted print

Figure 6 shows the zoom in surface finish produced by normal and assisted print. Standard print shows the lines are irregular which introduce a rough surface finish compared to ultrasonic and vacuum system assisted the lines are much more even.

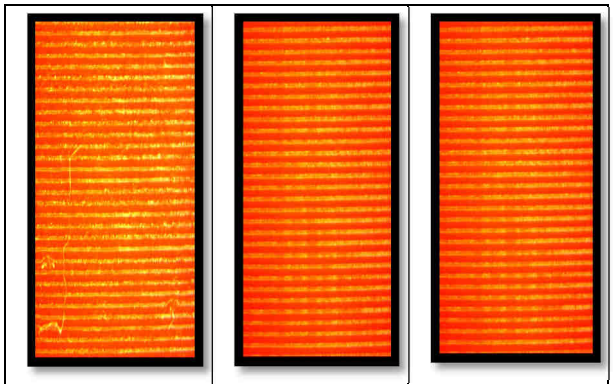

Figure 6 Zoom in surface finish

Surface finish related to thermal aspect because when the extrusion starts to extrude the semiliquid filament 200 degrees and above from one point to another, the polymer is rapidly cooled to room temperature. The temperature changes so rapid which lead to rough surface finish, there will be introducing to part distortion and stress which is undesirable to produce a fine and good surface finish quality; in this condition the shrinkage is unpredictable.

4. CONCLUSIONS

Ultrasonic energy is a mechanical vibration that occur when it is greater than 20kHz. When the ultrasonic energy interacts into the molten thermoplastic, the thermoplastic molecule will vibrate energetically. Thus, the vibration will produce a rise in temperature. When the thermoplastic from the extrusion is rapidly cooled to the room temperature for the molten polymer to solidify, it can reduce the rapid cooling. Ultrasonic energy absorption in thermoplastic melts cause a rapid rise in temperature. Vacuum occur when the air is removed from the chamber, means there will be no air particle inside the chamber. Hence, the heat can't transfer from one place to another because there is no medium for them to transfer. There for, the energy source from the nozzle part when it transferred to the 3D printer part, the heat energy will remain much longer and rapid cooling can be reducing. Consequently, it is obviously by adopting these two principals, it can help to overcome the limitation of the 3D printed parts.

ACKNOWLEDGEMENT

The authors are thankful to UTeM, UNISZA, and FRGS scheme no FRGS/1/2015/TK03/FKP/02/F00282.

REFERENCES

[1] I. Gibson, , Rosen, D.W. and Stucker, B. "*Additive manufacturing technologies*", Vol. 238, New York: Springer, 2010.

[2] L. Chua. K, F. Leong. K, and S. Lim. C, "*Rapid Prototyping: Principle and Applications*," 3rd ed., World Scientific, 2010.

[3] A. Boschetto and L. Bottini, "Roughness prediction in coupled operations of fused deposition modeling and barrel finishing," *J. Mater. Process. Technol.*, vol. 219, pp. 181–192, 2015.

[4] T. Tawakoli and B. A. Ã, "Influence of ultrasonic vibrations on dry grinding of soft steel," *Int. J. of Machine Tools & Manufacture* ,vol. 48, pp. 1585–1591, 2008.

[5] J. Avison, "The World of Physics," Nelson Thornes, 2014.

[6] W. Y. Loo and K. W. Loo, "*Sif Physics OI Tb*," South Asia: Pearson Education, 2007.

Proceedings of Innovative Research and Industrial Dialogue'16, pp. 7-8 (May 2017)

Investigation of heat transfer for vacuum system assisted fused deposition modeling: A finite element analysis

S. Maidin*, , J.H.U. Wong, A.S. Mohamed, W.F.A. Romlee, S. Akmal

Faculty of Manufacturing Engineering, Universiti Teknikal Malaysia Melaka, Hang Tuah Jaya, 76100 Durian Tunggal, Melaka, Malaysia

*Corresponding e-mail: shajahan@utem.edu.my

Keywords: Fused deposition modeling; vacuum system; finite element analysis

ABSTRACT – Fused deposition modeling was known to produce poor mechanical strength for functional parts due to the incomplete layer bonding. FDM machines are generally operated with or without enclosure. The enclosure system was found to produce more quality build but the results are not substantial due environmental inconsistencies. This paper aims to study the behavior of the heat transfer inside the enclosed vacuum system during FDM operations using finite element analysis. Simulation results showed that 5 inHg to 1 inHg can provide an ideal environment for FDM operations by limiting convective heating hence directly improving the parts mechanical strength.

1. INTRODUCTION

Fused deposition modelling is one the popular extrusion based AM technology [1]. What makes AM different from other conventional manufacturing are the capability to produce complex geometries and cavities [2]. As commonly used process in AM, FDM delivers easy operation, inexpensive machinery and elimination of tooling. Generally, FDM is more time and cost competitive in producing custom made products. In contrast, one of the restrictions to made functional parts is the inadequate strength of printed parts [3]. The strength is lower compared to part from injection moulding and extrusion process. The extruded filament solidified too fast for complete bonding to occur. Fast solidifications occurred when the heat is transferred from hot to a cold medium rapidly through conduction and convection process.

Vacuum technology has been used by various industries and studies to create an environment where low to ultra-high vacuum space exists. Vacuum is a void where there is no matter, a space that is empty with no particles. The atmospheric pressure is at 30 inHg (1 atm) containing particles of air constantly colliding with each other and transmitting energy from one to another. If there is no medium for them to travel, the energy cannot be transferred and remained at the place. Similarly, by reducing the atmospheric pressure, the air particles will reduce and particles can move freely with low chance of collisions [4]. Different vacuum pressure will produce a different thermal behaviour.

Heat is a form of energy that flows from one body to another body when there is a difference in temperature and stops when equilibrium temperature is achieved. Heat transfer of thermal energy happens through several ways; mainly thermal conduction, convection and radiation. This study focuses on convection, heat transfer in liquid or gaseous state. Convection will happen where there is a liquid or gaseous medium exists for heat transfer [5]. The change of density of fluid or gaseous will cause the motion of fluid.

In order to improve the layer by layer bonding, rate of cooling must be reduced and the solution is by applying operating FDM machine inside the vacuum system. This paper present a simulation study to observe the behaviour of heat transfer in vacuum environment and to investigate it's feasibility in FDM operations.

2. METHODOLOGY

This study requires the design of vacuum system using 3D CAD software. The system will have vacuum chamber, nozzle and heated bed. Other parts will be excluded in this study. Figure 2 shows of vacuum chamber with heated bed and nozzle.

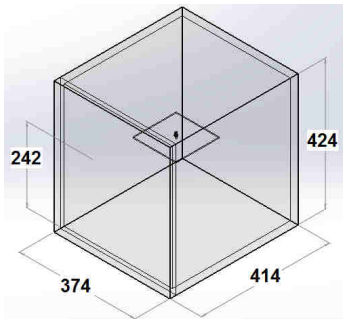

Figure 1 The vacuum chamber with nozzle and heated bed (mm)

Finite element analysis will be conducted using SolidWorks Flow Simulation. For the pre-preparations for the flow simulation, 3D CAD models of the chamber, nozzle and heated bed will be inserted. Input data are shown in Table 1.

Table 1 Input data for simulation

Input	Value
Simulation physical time (seconds)	3600
Time step interval (seconds)	60
Gravity (m/s^2)	-9.81
Air pressure (inHg)	30, 20, 10, 5, 1
Air velocity	Steady state
Air type	Laminar and

	turbulent
Wall condition	Adiabatic wall
Initial temperature (°C)	20.05 (default)
Constant Nozzle/Heat bed temperature (°C)	260/100

The result will be to observe on the contours, vectors and streamlines on how the heat travels inside the vacuum system during different pressure range.

3. RESULTS AND DISCUSSION

The results of finite element analysis are simulated and the cut plot results on 60th minutes are shown in Figure 2.

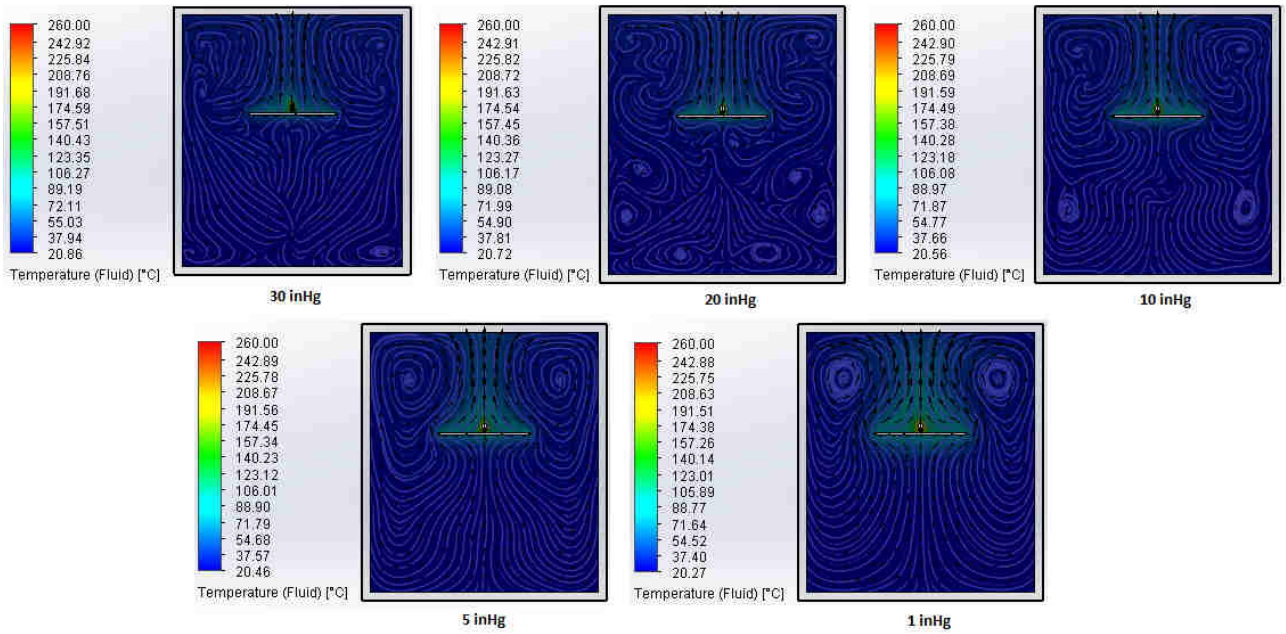

Figure 2 Thermal flows in 30, 20, 10, 5 and 1 inHg chamber

Figure 2 showed similar air flow dispersed from heat source upward, outward and downward. Hot air rises and draws cool air behind it. However, five different air flow patterns can be seen. Starting at 30 inHg, free mean path of the air particles is very small thus an irregular thermal flow can be seen due to the fact at atmospheric pressure, the particles create collisions. Here the irregularities will affect the quality of FDM parts. As the vacuum is increasing to 20inHg and 10inHg onwards, the air flow pattern began to change from turbulent to laminar flow. Parallel layers and regularities began to show. The free mean path is similar to the dimensions of the chamber. Optimum flow can be seen from 5 inHg to 1 inHg. The flow is smooth from both sides and almost parallel in each layer. Thermal flow rose up and down without disturbance hence would be an ideal pressure for FDM operations.

4. CONCLUSIONS

The efficiency of heat transfer is affected by air pressure. The lower the pressure, the heat transfer from the heat source to the cooler area can be reduced. The ideal environment for FDM operations are in between 5 inHg to 1 inHg. The flow lines are smooth and the heat transfer from the heat source is minimized as well. At vacuum, the reduction of medium of air particles caused inability for the heat to travel to the colder area. Hence, the heat will be maintained for a longer period of time which subsequently improves the layer bonding of FDM parts. Besides, a vacuum environment also provides clean environment free from dust and dirt. For future study, this paper needs to have actual experimentations to analyze the mechanical strength of vacuum-printed parts.

ACKNOWLEDGEMENT

The authors would like thank for the scholarship of 'Skim Zamalah UTeM' and Fundamental Research Grant Scheme (FRGS) grant number FRGS/1/2015/TK03/FKP/02/F00282.

REFERENCES

[1] I. Gibson, D. Rosen, and B. Stucker, *Additive manufacturing technologies: 3D printing, rapid prototyping, and direct digital manufacturing*, Springer, 2014.

[2] P. Deepa, "Fused deposition modeling – a rapid prototyping technique for product cycle time reduction cost effectively in aerospace applications," *IOSR Journal* , vol 5, pp. 62-68, 2014.

[3] H. Bikas, P. Stavropoulos, & G. Chryssolouris, "Additive manufacturing methods and modeling approaches: a critical review," *The International Journal of Advanced Manufacturing Technology*, vol 83, pp. 389-405, 2016.

[4] J.F. O'Hanlon, *A user's guide to vacuum technology*. John Wiley & Sons, 2005.

[5] J. Whitaker, *Power vacuum tubes handbook*. CRC press, 2012.

Proceedings of Innovative Research and Industrial Dialogue'16, pp. 9-10 (May 2017)

Designing and implementation of automated room temperature control system to optimize energy consumption in a building

J.S. Quah[1], K.A.M. Annuar[2,*], M.F. Miskon[1], M.H. Harun[2], M.F.M.A. Halim[2]

[1)]Faculty of Electrical Engineering, Universiti Teknikal Malaysia Melaka, Hang Tuah Jaya, 76100 Durian Tunggal, Melaka, Malaysia.

[2)]Faculty of Engineering Technology, Universiti Teknikal Malaysia Melaka, Hang Tuah Jaya, 76100 Durian Tunggal, Melaka, Malaysia.

[*]Corresponding e-mail: khalilazha@utem.edu.my

Keywords: Automatic control system; indoor environment management, energy saving

ABSTRACT – As society enters the 21st century, an increasing amount of work is now being done in an office where a multitude of cooling appliances are used to maintain the overall temperature of the office. However, it is simply energy inefficient to leave all the appliances on all the time as the amount of people vary and so too does the need for said appliances to be on throughout the day. Thus in this paper, we have designed and implemented room cooling/heating system that is capable of incorporates all cooling/heating elements in the room and hence turning them on or off automatically in an effort to maintain a preset temperature of the users choice.

1. INTRODUCTION

Energy conservation is an emerging issue or topic for humanity as the backlash from our past and current over reliance on fossil fuel. The best thing that can be done now would be to reduce the power consumption pre-capital so that we can start the process of changing our dependency from non-renewable to renewable energies. It was found in a previous study that approximately 60% of all energy generated globally is used for residential, commercial and industrial purposes and half of it is used specifically for space heating and cooling only [1, 2] hence it would be safe to assume that a reduction in energy consumption within this division itself would be able to reduce the overall energy consumption by a significant amount.

By merely removing cooling element would not be a viable option as it would directly affect the quality of works as well as quality of life of the employee themselves [3]. Instead, a better idea would be to connect all existing heating and cooling elements within the room using the internet of things [4] and mapping out the possible heat transfer interaction between itself and its surroundings so that an automated system can automatically can optimally determine the appliances that needs to be turn on so that optimum temperature for thermal comfort can be achieve [5, 6] at any given time of the day or whenever it should be on in the first place i.e. presence of people in the room hence indirectly reducing the amount of energy consumption.

2. METHODOLOGY

To make idea into a working system, the project was broken down into 2 parts where the 1st part is regarding the algorithm which determines the optimum configuration of what appliances that needs to be turned on at any given time to achieve the desired temperature or whenever to turn all the appliances off because there is nobody in the room for a long time as seen in figure 1.

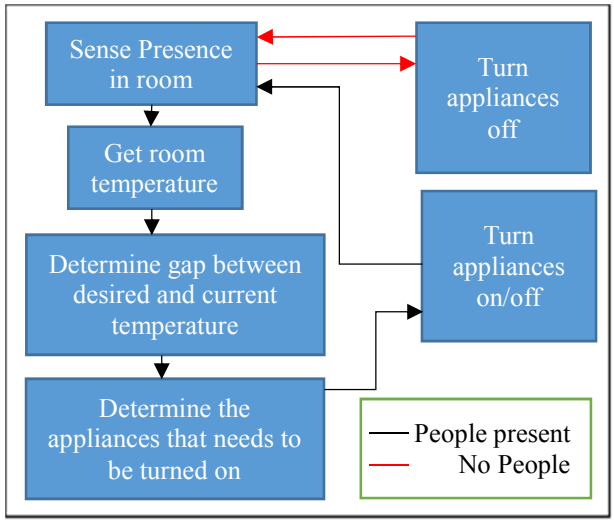

Figure 1 Expected algorithm operation

For the second part deals with the hardware implementation. To implement said system, an Arduino UNO was used as the microcontroller. Said microcontroller would then be connected to HC-05 and multiple HC-06 Bluetooth module to facilitate the transfer of data from the main controller hosting the algorithm to the slave controller which turns the appliances on or off or to relay information back to the main controller such as indoor and outdoor temperature or presence of people without the need of a vast array of wires sprawling throughout the room as seem in figure 2. Arduino's ability to read voltage levels allows for a method to control the AC frequency value via computations [7], furthermore, with minor additions of either cameras or Arduino motion sensor is more than capable of counting the number of people in the room [8].

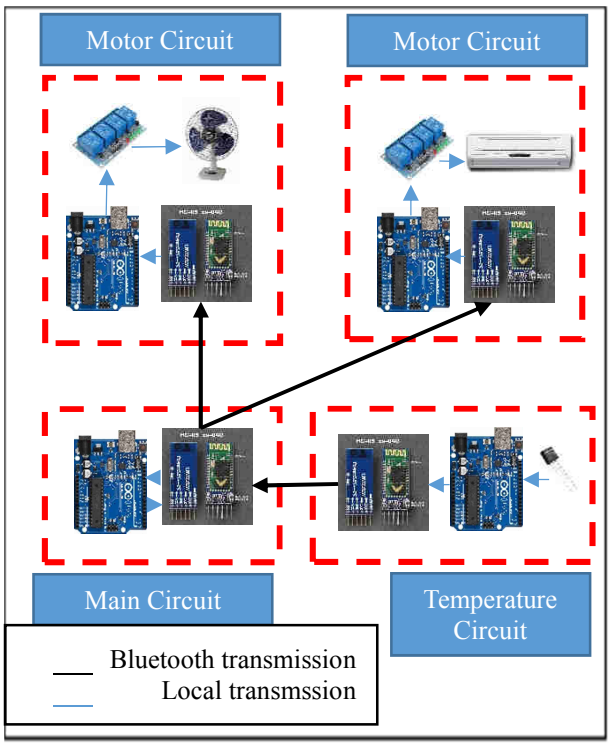

Figure 2 Schematic of hardware communication

3. RESULT

For this project, a simulation comparing the performance of the designed system against UTeM's air-conditioning policy when connected to an air conditioner and a fan can be seen in Figure 3 & 4.

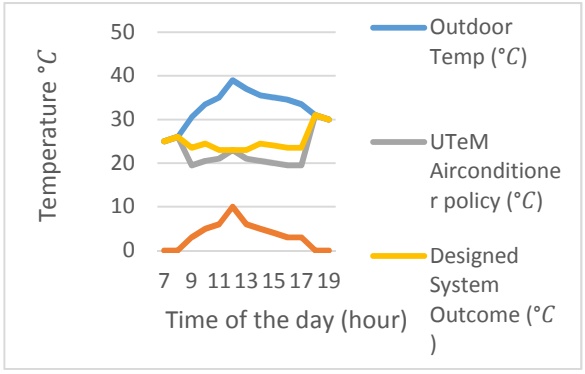

Figure 3 Comparison between the standard systems temperature outcome with the designed system outcome

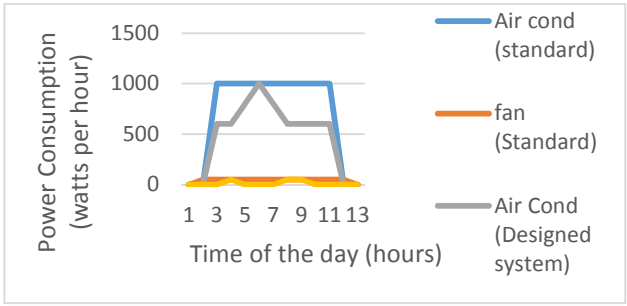

Figure 4 Comparison of possible power consumption between standard procedure and designed system procedure

By comparing the power consumption for UTeM's air conditioning policy which turns the central air Cond at maximum at 9am and turns it off at 5pm the total watt consumption of the day would be total up into an estimate of 9550 watts whereas when implementing the designed system, because the air Conditioner output is varied based on the amount of people present, the power consumption has been predictably reduced to an estimate of 6350 watts which is a 35%

4. SUMMARY

From the results, by implementing this system which first integrates various cooling elements in the room and then controlling each of those elements in order to achieve a predetermined temperature, it would be possible to reduce overall energy consumption by 35%.

ACKNOWLEDGEMENT

The authors would like to thanks for the support given to this research by Ministry of Higher Education Malaysia and Universiti Teknikal Malaysia Melaka (UTeM) for support this under RAGS RAGS/1/2015/TK0/FTK/03/B00118 project.

REFERENCES

[1] J. Lausten, "Energy Efficiency Requirements in Building Codes", Energy Efficiency Policies for New Buildings. Paris,France: International Energy Agency, 2008

[2] K. Wongpatikaseree, T. Okada and Y. Tan, "Analysis of the thermal comfort and power consumption in apartment domain," *2015 IEEE 4th Global Conference on Consumer Electronics (GCCE),* Osaka, 2015, pp. 423-426.

[3] L. Amoo, H. A. Guda, H. A. Sambo and T. L. G. Soh, "Design and implementation of a room temperature control system: Microcontroller-based," *2014 IEEE Student Conference on Research and Development (SCOReD),* Batu Ferringhi, 2014, pp. 1-6.

[4] Z. Babovic, J. Protic, V. Milutinovic, "Web Performance Evaluation for Internet of Things Applications," *IEEE Access*, vol 4, pp.6974-6992, 2016.

[5] S. M. Buhari, N. J. Tuah, K. O. Chong, S. G. Lim and A. G. Naim, "Fuzzy based room temperature control by integrating sensors and cameras with a grid," *2013 IEEE Symposium on Computational Intelligence for Communication Systems and Networks (CIComms),* Singapore, 2013, pp. 61-65.

[6] N. Kopmann, R. Streblow and D. Müller, "Test of new control strategies for room temperature control systems fully controllable surroundings for a heating system with radiators," *2015 International Conference on Smart Cities and Green ICT Systems (SMARTGREENS)*, Lisbon, Portugal, 2015, pp. 1-6.

[7] M.F.M. Ab Halim, M.H. Harun, K.A.M. Annuar, S. Ahmad, M.H.B.C. Hasan "Measurement of low frequency signal of power grid using Arduino" *2015 IEEE Conference on Energy Conversion,* 2015, pp. 96-101.

[8] M. F. Mohd Ab Halim, M. H. Harun, K. A. Mohd Annuar and S. Ahmad," Monitoring Grid Frequency" *ARPN Journal Of Engineering And Applied Sciences*, vol. 10, no. 18, pp.8413-8416, 2015.

Proceedings of Innovative Research and Industrial Dialogue'16, pp. 11-12 (May 2017)

Static Torque Profile of Switched Reluctance Actuator

I.Yusri[1], M.M.Ghazaly[1*], M.F.Rahmat[2], I.W. Jamaludin[1], Z.Abdullah[3], R.Ranom[1]

[1]Center for Robotics and Industrial Automation (CeRIA), Faculty of Electrical Engineering, Universiti Teknikal Malaysia Melaka, Hang Tuah Jaya,76100 Durian Tunggal, Melaka, Malaysia.

[2]Faculty of Electrical Engineering, Universiti Teknologi Malaysia, 81310 UTM Johor Bahru, Johor, Malaysia.

[3] Faculty of Manufacturing Engineering, Universiti Teknikal Malaysia Melaka, Hang Tuah Jaya,76100 Durian Tunggal, Melaka, Malaysia

[*]Corresponding e-mail: mariam@utem.edu.my

Keywords: Electromagnetic; actuator; finite element method

ABSTRACT – This paper presents the static torque profile of Switched Reluctance Actuator (SRA) based on different rotor's position. The analysis was done by using Finite Element Method (FEM) through computational software. In order to achieve high torque value, the developed design of SRA was according to the optimized parameter. The excitation current was varied from 0 to 2A at Phase A only. The rotor has a tendency to rotate towards specific direction depends on it's initial position. The FEM result shows that the maximum positive and negative torque achieve were 122.54 mNm and -111.69 mNm respectively which represents the direction rotation.

1. INTRODUCTION

Actuator is a type of motor that is responsible for moving in linear or rotary. It is operated by various type of sources such as electric current, hydraulic fluid or pneumatic pressure. Most of the recent research work have been focused on the electromagnetic actuator that is adopted rare earth permanent magnet material [1], [2]. Unfortunately, permanent magnet has several drawbacks such as high cost and non-environmental friendly. Switched Reluctance Actuator (SRA) is one of the candidates for rotary electromagnetic actuators which comparable with Permanent Magnet machines. SRA has several advantages such as simple structure, low cost, compact and maintenance free [3]. It has the potential to generate high torque and positioning accuracy based on the design [4]. It is usually employed in precision applications like Pick-and-Place (P&P). However, there are few problems in SRA such as; (a) low torque for its volume; (b) low efficiency; (c) noise, vibration and torque ripple.

Previous research work conducted by Piyush et al. [5] has presented the static torque profiles for a given design. The test was made at specific single phase to study its characteristic. Therefore, this paper will analyze the optimized design of SRA on static torque profile by considering the position of the rotor. It is important to determine the relationship of static torque and rotor's position towards the direction of rotation.

2. METHODOLOGY

The torque characteristic is a function of excitation current and the rotor position. Since the simulation was done without regards to continuous rotation, the result was represented static torque of the actuator. Maxwell 3D software is used to design and analyze the electromagnetic actuator which applied finite element analysis. This is a high-performance software which uses finite element analysis. The parameter used to develop the actuator is as shown in Table 1. These parameters have gone through optimization process accordingly to achieve high torque value.

Figure 1 shows the geometry design of the SR actuator. The actuator was designed with stator to rotor, S:R pole ratio=6:4 using the material of Low Carbon steel (Steel 1008). The SR actuator is operated with the 3-phase system. However, in order to analyze the torque profile of single phase, the current was excited at Phase A only with 0 to 2A at an interval of 0.5A. The simulation was done by rotating the rotor 80° anticlockwise. Figure 2 illustrate the rotor travelling from unaligned position (0°) between rotor and stator to unaligned position passing the stator's pole (80°). The resulted torques for each interval of 2° are recorded.

Table 1 Labelling and dimension of SR actuator

Labelling		Dimension	
Phase A		Stator outer diameter, Do	60 mm
Phase B		Stator inner diameter, Di	31.8 mm
Phase C		Rotor diameter, Dir	31.6 mm
Stator		Stator and rotor height, H	36 mm
Rotor		Air gap thickness, G	0.2 mm
		Winding number	60 Turn
		Stator : Rotor arc angle, β_s:β_r	29° : 40°
		S : R pole ratio	6 : 4

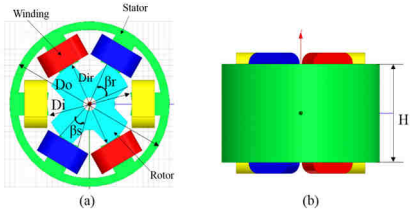

Figure 1 Geometry design of S:R=6:4 pole ratio configuration (a) top and (b) side view

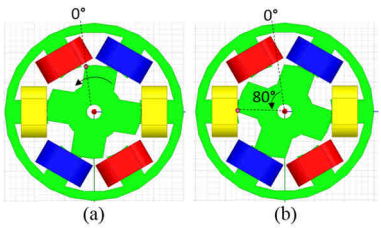

Figure 2 Rotor position for Phase A with single excitation current 2A (a) initial, 0° and (b) final, 80°

3. RESULT AND DISCUSSION

SR actuator operation principle is due to the tendency of the magnetic flux to have low reluctance pathway. Air is one of the medium that has high reluctance compare to Low Carbon steel that has much lower reluctance. If the position of the rotor's pole is away from the stator's pole (unaligned position), the magnetic flux has to cross the large air gap which will result in low torque. Thus, the position of the rotor will be a crucial part on determining the value and polarity of torque.

Varying the position of the rotor resulted in different static torque value. Since torque has a sense of motion's direction, it will shift from positive torque to negative torque according to the assigned position. Based on Figure 3, the first 34° of rotation generated only positive static torque. This is due to the tendency of the rotor to move anticlockwise base on the given torque. As it travels further, the resulted torque began shifting to a negative value. At this position, the rotor tends to move clockwise.

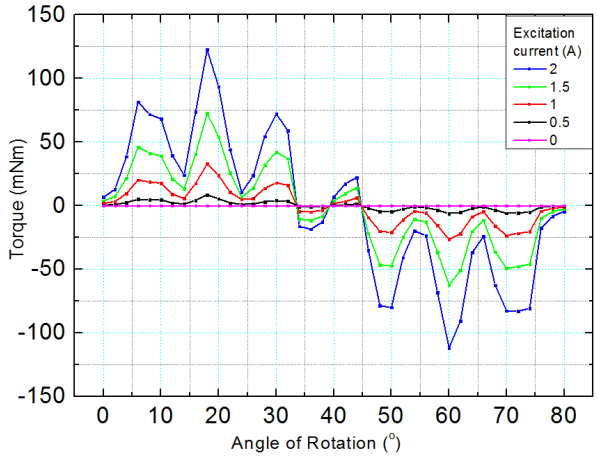

Figure 3 Static torque profile of designed SRA

The highest positive torque with 2A excitation current was achieved at position of 18° with a value of torque 122.54 mNm. Meanwhile, the highest negative torque is -111.69 mNm at position 68°. Both positive and negative torque have 13° and 14° overlapping position which is approximately identical. Thus, the torque value also almost equivalent but in different polarity. This position neither high reluctance nor saturated. It has enough space for enabling accumulate magnetic flux to flow and generate high torque.

As it rotates further, the generate torque is reduced. Saturation level is reached when the rotor and stator pole is aligned. The magnetic flux is effortlessly passed through both poles. However, there are still a small amount of generated torque exist during the saturation level. This is because the particular position assigned was not fully centered. It does have slightly deviated.

4. CONCLUSIONS

As a conclusion, torque production by the SR actuator is based on the change of reluctance with respect to the position of the rotor. When the rotor approaches aligned position, the static torque began to increase. However, further increase of rotation will lead to saturation effect and decrease the torque generated. Both the highest positive and negative torque with maximum excitation current are almost identical which is 122.54 mNm and -111.69 mNm as the overlapping degree is alike. The polarity of the torque represents the direction rotor that will rotate at the particular position. The static torque profile are nearly same for each excitation current value. It is essential to determine the relationship of torque and position for developing the phase switching of excitation current in future research.

ACKNOWLEDGEMENT

Authors are grateful to Universiti Teknikal Malaysia (UTeM) and UTeM Zamalah Scheme for supporting the research. This research and its publication are supported by Research Acculturation Collaboration Effort (RACE) grant no. RACE/F3/TK5/FKE/F00249 and the Fundamental Research Grant Scheme (FRGS) no. FRGS/1/2016/TK04/FKE-CERIA/F00305.

REFERENCES

[1] S. Fang, K. Guo, H. Lin, D. Wang, and H. Yang, "Electromagnetic Analysis of a HTS Linear-Rotary Permanent Magnet Actuator," *IEEE Trans. Appl. Supercond.*, vol. 26, no. 7, 2016.

[2] K.J. Meessen, J.J.H. Paulides, and E.A. Lomonova, "Analysis of a Novel Magnetization Pattern for 2-DoF Rotary-Linear Actuators," *IEEE Trans. Magn.*, vol. 48, no. 11, pp. 3867–3870, 2012.

[3] T. J. Teo, H. Zhu, S. Member, and S. Chen, "Principle and Modeling of A Novel Moving Coil Linear-Rotary Electromagnetic Actuator," *IEEE Trans. Ind. Electron.*, vol. 0046, no. c, 2016.

[4] I. Yusri, M. Md Ghazaly, E. A. Ali Alandoli, M. F. Rahmat, Z. Abdullah, M. A. Md Ali, and R. Ranom, "Optimization of The Force Characteristic of Rotary Motion Type of Electromagnetic Actuator based on Finite Element Analysis," *Jurnal Teknologi*, vol. 9, no. 1, pp. 13–20, 2016.

[5] P. C. Desai, M. Krishnamurthy, N. Schofield, and A. Emadi, "Switched reluctance machines with higher rotor poles than stator poles for improved output torque characteristics," *Proceeding IEEE Ind. Electron 2009.*, no. 1, pp. 1338–1343.

Proceedings of Innovative Research and Industrial Dialogue'16, pp. 13-14 (May 2017)

Design and control leg-exo robot for rehabilitation purpose

S.A. Ali[1], K.A.M. Annuar [2,*], M.F. Miskon[1], M.H. Harun[2], M.F.M. Abdul Halim[2]

[1)]Faculty of Electrical Engineering, Universiti Teknikal Malaysia Melaka, Hang Tuah Jaya, 76100 Durian Tunggal, Melaka, Malaysia.
[2)]Faculty of Engineering Technology, Universiti Teknikal Malaysia Melaka, Hang Tuah Jaya, 76100 Durian Tunggal, Melaka, Malaysia.

[*]Corresponding e-mail: khalilazha@utem.edu.my

Keywords: Exoskeleton control; motor modelling; trajectory polynomial

ABSTRACT – Development lower body exoskeleton robot for assistance and rehabilitation is challengeable active field in robotics. The research contributes in developing wearable robotic leg which can help people in their rehabilitation process. Apart from the exoskeleton structure, the challenge is on how to control the exoskeleton so that it will track human walking movements while at the same time provide additional power to the motions with stability and accuracy. The implementation of the project will be divided into simulation via matlab, vrep software and hardware. Besides the robotics equations, the controlling will involve PID controller and disturbance observer.

1. INTRODUCTION

The exoskeleton robots are introduced to help patients in their rehabilitation treatment. These kinds of robots divided in two parts, the upper limb and the lower limb of the body. The review present robotic systems that exist previously to solve problems in damaged parts of the lower limb of human's body, such as the knee, the ankle and the hip. All of these systems were generally created to do specific function to help people who have permanent injuries due to strokes or accidents in their therapy to regain the walking ability. Research on exoskeleton can be seen in many research papers. According to Gong Chen et al [1], review and analysis some of exoskeleton model on their mechanical design, movement system and integration control algorithm. There is also discussion on the limitation and technical challenges development of the model [1-2]. The previous lower body exoskeleton is shown in Figure 1.

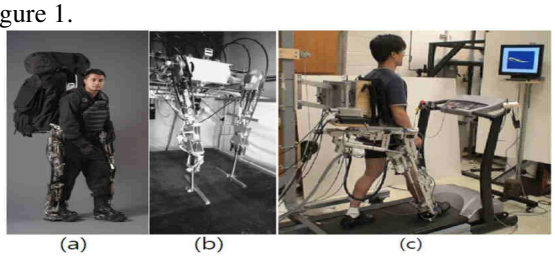

Figure 1 Previous exoskeleton systems a) Bleex,b) Lopes and c) Alex

The first field-operational lower extremity exoskeleton ever developed comprised of two powered anthropomorphic legs, a power unit, and a backpack-like frame on which a variety of heavy loads can be mounted. This system provides its wearer with the ability to carry significant loads on his back with minimal effort over any type of terrains. The overall concept of this lower extremity exoskeleton is that the human provides an intelligent control system for the exoskeleton while the exoskeleton actuators provide most of the strength necessary for walking [3]. The mechanical structure design can be fit or adjusted with the characteristics of the human body. The design and structure is supposed to be light when the models are developed for the elder people. One of the essential objective in the design of these custom vest allowing the joints' moving angle of robots should be identical to the force and motion of human joints as much as possible and good safety [4-5]. Exoskeleton control requires a totally opposite goal from classical and modern control theory: maximize the sensitivity of the closed loop system to forces and torques. The design goal states that the exoskeleton controller needs a large sensitivity to forces and torques. Obtaining a good model of each exoskeleton link is not hard since the designer can control their dimension and construction. However, obtaining a good model of torso is nontrivial because the torso includes a variable payload [6].

Asynchronous exo-leg movement is defined as a condition where the walking movement (motion) profile of the lower body exoskeleton robot and human wearer are asynchronous. In biomechanical field, several models have been determined through observation of human walking movement. However, the suitable performance on asynchronous leg-exo movement on the lower body exoskeleton robot is unknown and has not been validated yet.

2. SIMULATION AND HARDWARE

This paper focuses on Building a lower body exoskeleton model. The project use Vrep and Matlab (Simulink) as software programs to simulate the model as well as to validate the effectiveness of the control strategy.

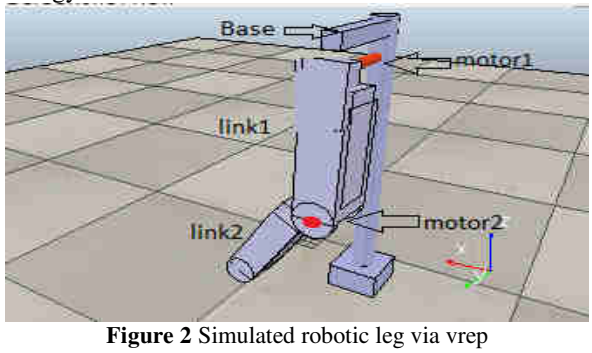

Figure 2 Simulated robotic leg via vrep

The hardware is built using geared DC motors, motor drivers, encoders and micro-box. The derived

model will be evaluated and implemented on the actual lower body exoskeleton structure.

3. METHODOLOGY

The methodology of the project begins with simulating the human walking and transforms it to equations. Trajectory planning is an important part in robotics. It is used to design a path for an electrical motor or a manipulator to move to a desired movement with specific velocity and acceleration. We have using quantic equation to represent the human walking to equation as in 1, 2 and 3.

$$\Theta(t) = a_0 + a_1 t + a_2 t^2 + a_3 t^3 + a_4 t^4 + a_5 t^5 \quad (1)$$

$$V(t) = a_1 + 2a_2 t + 3a_3 t^2 + 4a_4 t^3 + 5a_5 t^4 \quad (2)$$

$$a(t) = 2a_2 + 6a_3 t + 12a_4 t^2 + 20a_5 t^3 \quad (3)$$

3.1 Dc motor modelling

Table 1 Geared DC motor parameter

Parameter	Value	Parameter	Value
R	0.16ohm	ki	20mN/A
L	45µH	J	120gcm^2
Kb	2.08mVmin		

Using parameters in table 1, the transfer function can be developed to get stable system. Yet the system is not ready to be used in the robotic leg unless we use PID controller. Figure 3 shows the function of the motors with PID. The transfer function is derived from Table 1.

$$G(s) = \frac{0.02}{s(5.37\times10^{-10}s^2 + 2\times10^{-6}s + 2.2\times10^{-3})} \quad (4)$$

Table 2 PID controller parameters

Parameter	Value
Kp	0.22579
Ki	0.01238
Kd	0.05413

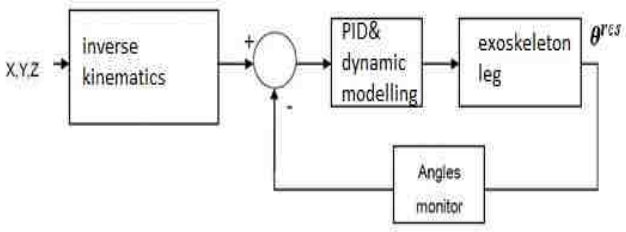

Figure 3 Exo-leg block diagram

The dynamic modeling is derived from the fundamental motion equation as shown in equation 5. M(q) is the mass matrix, V(q,q) is the velocity matrix and g(q) is gravity matrix.

$$M(q)\ddot{q} + V_m(q,\dot{q})\dot{q} + G(q) = \begin{bmatrix} \tau_1 \\ \tau_2 \end{bmatrix} \quad (5)$$

4. RESULT AND DISCUSSION

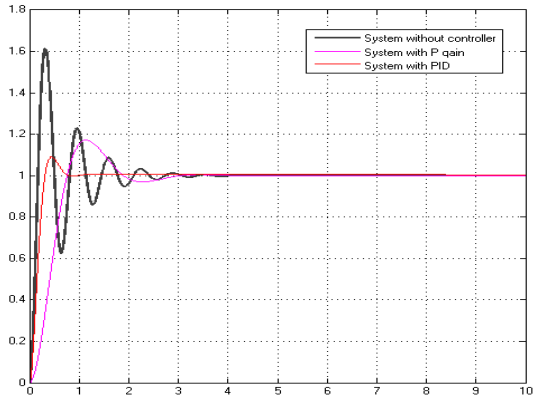

Figure 4 Motor modeling response

Equation 5 and other more equations are used to control the robotic leg motion by controlling the torque and the current. The current will be reduced in the motors due to variables not mentioned here. Because of that the current is fed back to keep it at constants value which lead to stable process

ACKNOWLEDGEMENT

The authors would like to thanks for the support given to this research by Ministry of Higher Education Malaysia and Universiti Teknikal Malaysia Melaka (UTeM) for support this under RAGS RAGS/1/2015/TK0/FTK/03/B00118 project.

REFERENCES

[1] G. Chen, C. K. Chan, Z. Guo, and H. Yu, "A Review of Lower Extremity Assistive Robotic Exoskeletons in Rehabilitation Therapy," *Critical Reviews™ in Biomedical Engineering*, vol. 41 no.4-5 pp. 343-363, 2013.

[2] N. Li, L. Yan, H. Qian, H. Wu, J. Wu and S. Men, "Review on Lower Extremity Exoskeleton Robot," *The Open Automation and Control Systems Journal*, vol. 7, pp. 441-453, 2015.

[3] J. Kazerooni, H. Racine, J.-L. Huang, and R. Steger, "On the Control of the Berkeley Lower Extremity Exoskeleton (BLEEX)," in *Proceedings of the 2005 IEEE International Conference on Robotics and Automation*, 2005, pp. 4353-4360.

[4] S. Song, "The Lower Extremity Walking Assist Mechanism Design and Simulation Research", Shen Yang Aerospace University, China, 2013.

[5] H. Yu, Manolo STA Cruz, G. Chen, S. Huang, C. Zhu, E. Chew, Y. S. Ng, and N.V. Thakor, "Mechanical Design of a Portable Knee-Ankle-Foot Robot," in *2013 IEEE International Conference on Robotics and Automation (ICRA)*, 2013, pp. 2175-2188.

[6] S. Kim, G. Anwar, and H. Kazerooni, "High Speed Communication Network for Controls with Application on the Exoskeleton", in *Proceeding of the 2004 American Control Conference*, 2004, pp. 355-360.

Proposed framework of biomimetic features database system to aid product conceptual design

W.F.A. Romlee, S. Maidin*, J.H.U. Wong, A.S. Mohamed, S. Akmal.

Faculty of Manufacturing Engineering, Universiti Teknikal Malaysia Melaka, Hang Tuah Jaya, 76100 Durian Tunggal, Melaka, Malaysia

*Corresponding e-mail: shajahan@utem.edu.my

Keywords: Bio-inspired design; database; design

ABSTRACT – This paper presents a proposed framework of a biomimetic features database system. The database is intended as a tool to aid and inspire designers in implementing nature element at product conceptual design stage. It is created by developing a framework that can ease designer to relate biomimetic information to product design. Next, the data is uploaded into MySQL database management system while Microsoft Visual Studio is used to create the system web applications. The user interface design is considered very thoroughly as the success of this system relies heavily on user acceptance. Finally, the information retrieval process of the proposed database is being explained.

1. INTRODUCTION

Biomimetics refers to contribution or imitation of idea from nature which is then being transferred to technology as stated in previous study [1]. Eggermont [2] found that despite the successful inventions of biomimetic like Velcro from burdock leaves, most designers neglect biomimetic in solving design problems due to the scattered information of design from nature. Moreover, traditionally biomimetics requires product designers to have both understanding of engineering and biological system that increases the intricacy of the design process as stated in previous study [3]. Other than that, there are lacks of visual examples from nature to aid in product design process.

Only in recent years, systematic approaches have been developed to aid in biomimetic product design. However, Maidin et. al. [4] stated that there are still limitations in the usage of available biomimetic tool that makes this concept less favourable to designers. Therefore, this paper presents the framework proposal for development of a database to support product design with the emphasis on to embed design idea from nature at conceptual design stage.

The development of biomimetic features database system is conducted in phases. This proposal is of initial stage of the process where framework taxonomy and flow of the database are developed. The next phase involving tests for usability of the database by potential users is not covered in this paper.

2. METHODOLOGY

In order to develop the database, firstly studies conducted by previous researchers are reviewed. Characteristics of available tools are first identified to propose for the development of a new biomimetic tool. The result can be summarized as in Table 1.

Table 1 Summary of biomimetic tools

Tools	Descriptions	Limitations	Ref.
IDEA INSPIRE and DANE Databases	Present biomimetics information in a form of database.	Requires access to certain software and entry size is limited.	[4]
Asknature Website	Open access website based on Biomimicry Taxonomy.	Broad classification but not closely represent engineering design.	[4]
Natural Language Analysis	Search biological text based on Natural Language Transforma-tion using verb keyword .	Requires access to certain software and fixation exists on some biological phrases results in difficulty to match to other field.	[4]

Based on the findings, it is necessary to provide user with a biomimetic design tool that is user- friendly, with open access and consist of wide range of entries that relate biomimetic information to product design.

Next, a framework is developed to sort the scattered biomimetic information in an orderly manner to ease retrieval of beneficial biomimetic information for product conceptual design. The framework is built by classifying biomimetic products based on their respective functions. MySQL was used as database management system whereas Microsoft Visual Studio was used to create the system web application.

3. RESULTS AND DISCUSSIONS

3.1 Database Framework Taxonomy

The biomimetic framework taxonomy developed is shown in Table 2.

Table 2 Biomimetic framework taxonomy

Buoyancy	Products that implement nature to enable its floating properties.
Aerodyna - mic	Products that imitate nature in handling drag force and lift.
Attachment	Products that attach substances using inspiration from biological principles.
Noise reduction	Products that reduce its operating noise by implementing biological phenomena.
Drag reduction	Application of biological principles to reduce drag and improve movements in products.
Weight-Countering	Use of biological concept to manage product weight and improve function.
Light and Display	Application of light absorption, refraction and reflection in nature that improve product display and imaging.
Construction	Improvement of products using biological principles involving construction and infrastructure.
Stain resistant	Products that resist stain by implementing biological principles.
Self-cleaning	Products that apply self - cleaning concepts as of biological phenomena
Energy efficiency	Products that reduce energy usage by implementing biological principles.

3.2 Retrieval of Information Process

The process flow of the biomimetic information in the database is as in Figure 1.

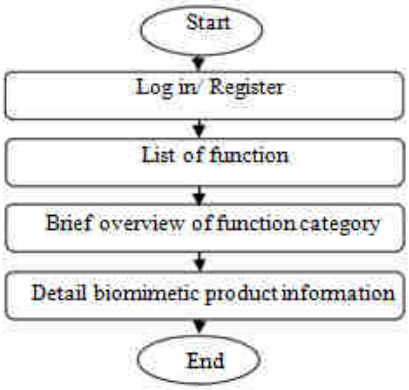

Figure 1 Database flow

First, the database user will encounter the introduction page where the aim, function and overall content of the database are stated. Since the database is under development, new user is required to register their contact details to obtain feedback for improvement of the database in the future. The log in requirement is very simple since it only requires email of user.

Next, the framework category is displayed to aid designers in information retrieval process. Since designers usually have their desirable product function, it is easier for them to identify useful biomimetic information by having this framework. As an example, an aircraft engineer might want to improve the aerodynamic properties of an airplane. By having this database, he can simply click on the aerodynamic category and view related information for design inspiration.

After the function has been chosen, the user can view biomimetics products under the category with some explanation as shown in Figure 2.

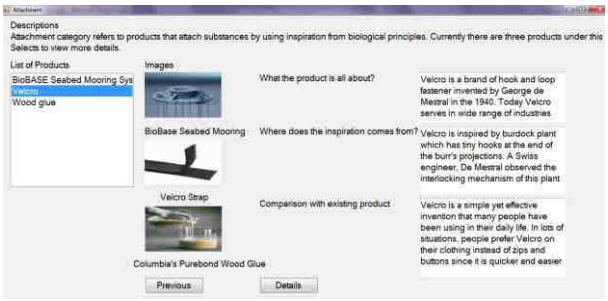

Figure 2 Function overview page

When the user is interested to know more about the product, the detail pages will reveal relevant helpful information and images. Besides, user can also add and store information to the database.

4. CONCLUSIONS

Biomimetic is not new in product design. However, the biomimetic is rarely referred in designing a product at the conceptual stage. In order to make use of the nature elements at the conceptual design stage, this framework was proposed with characteristics that can fulfill user requirements and counter problems that arise regarding previous methods or tools. This paper presents the framework and process flow of the database. In the next stage, test will be conducted using case study of product design to identify the effectiveness and usability of the database.

ACKNOWLEDGEMENT

Authors would like to acknowledge the financial support from '*Skim Zamalah UTeM'* and Fundamental Research Grant Scheme grant number FRGS /1/2015/ TK03/FKP/ 02/F00282.

REFERENCES

[1] T. Speck and O. Speck, *Process Sequences in Biomimetic Research*. WIT Press; 2008.

[2] M.J. Eggermont, *Biomimetics as Problem-solving, Creativity and Innovation Tool*, WIT Press; 2008.

[3] M.W. Glier, J. Tsenn, D.A. McAdams and J.S. Linsey, "Evaluating Methods for Bioinspired Concept Generation", in *Design Computing and Cognition DCC'12*, 2012.

[4] S. Maidin , W.F.A. Romlee, A.S. Mohamed, N.M.A.N. Mohammad, J.H.U. Wong, S. Akmal, "Tools To Incorporate Biomimetic Into Product Design - A Review" in *5th International Conference on Design and Concurrent Engineering),* 2016.

Proceedings of Innovative Research and Industrial Dialogue'16, pp. 17-18 (May 2017)

Experimental investigation of the motion characteristics for a passive quarter car suspension system

S.P. Tee, M.M. Ghazaly*, S.H. Chong, I.W. Jamaludin

Center for Robotics and Industrial Automation (CeRIA), Faculty of Electric Engineering, Universiti Teknikal Malaysia Melaka, Hang Tuah Jaya, 76100 Durian Tunggal, Melaka, Malaysia

*Corresponding e-mail: mariam@utem.edu.my

Keywords: Quarter car model; passive suspension system; PTP positioning

ABSTRACT – This research paper discussed the study of a two degree-of-freedom quarter car model passive suspension system. An open loop experiment characteristics using system identification method were carried out to determine the transfer function of the passive suspension system. Once these steps are completed, a closed loop compensated system is designed to control the position of Platform 1; i.e. the road surface. Platform 1 will provide the road profile of different step height for the passive quarter car suspension system. The PID controller is proven to be able to improve steady-state error by 48.6% and 21.8% for reference heights of 30cm and 36cm respectively, with a slight 12% overshoot for 36cm reference height.

1. INTRODUCTION

Design engineers are constantly on a lookout for improvements to reduce shocks in vehicles due to irregular road surfaces, drag forces and engine vibrations. Vehicle suspension system play an ultimate role, to increase car handling and comfort by reducing and isolating shock applied to the vehicle. Suspension system is categorized into 3 types, which are passive suspension system, active suspension system and semi-active suspension system [1].

Sharma et al. [2] experimented on the performance of an automotive passive suspension system using a quarter car model and discovered the system is unsatisfactory. Active suspension system with pneumatic actuators is concluded to improve ride comfort and maintains vehicle handling, compared to a passive suspension, as previous study [3].

The performance of passive suspension and active suspension is investigated using 2 different control algorithms, "Skyhook stability augmentation system (Sky-SAS)" algorithm and "stability augmentation system (SAS)" algorithm, as previous study [4].

A low cost and simple semi-active suspension system is proposed and showed to provide great damping properties, in the meantime reducing the compromise of comfort and handling issue faced by passive suspension [5]. The modelling is based on equations of motion that includes different parameters such as damping ratio, stiffness and displacement. The evaluation is done via simulations only by transforming the equations into a data flow circuit in MATLAB/Simulink, then generating the graphical outputs.

2. METHODOLOGY

Figure 1 shows the experimental setup of the Passive Quarter Car Suspension System. Figure 1 shows Platform 1 represents the road surface which a car is moving on. Different input to the double acting cylinder will move Platform 1 by different magnitude and displacement, imitating the different road profiles when cars are moving in various terrains. Platform 2 represents the car tire while Platform 3 is the car body which different weights can be added to signify different car masses. The transfer function of the car suspension system is given by Equation 1.

$$\mathrm{TF} = \frac{-2.771s + 110}{s^2 + 47.18s + 4.467} \quad (1)$$

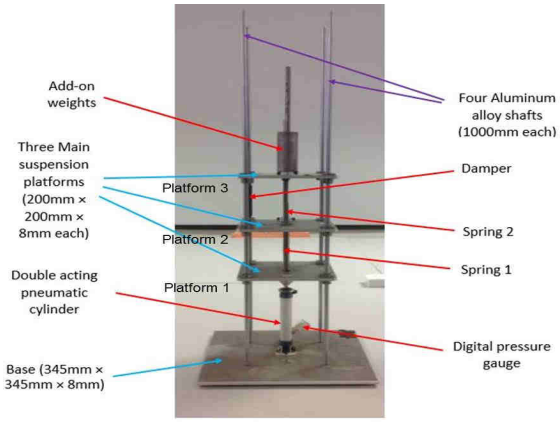

Figure 1 Structure and setup of passive suspension system

3. RESULTS AND DISCUSSION

In order to evaluate the control performances of the car suspension system, the PID controller was applied as shown in the block diagram in Figure 2. Initially the value of K_p was varied, while setting the K_i and K_d values to 0, this is also known as a proportional (P) controller. In this paper, the final values of the PID controller was set to $K_p = 1.35$, $K_i = 0.021$, $K_d = 0.0022$. The experiments are evaluated at reference height 30cm and 36cm respectively. Figure 3 and Figure 4 show that the PID controller able to reduced steady-state errors, to 0.37cm and 0.43cm for the experimental value. Table 1 and Table 2 show the performances of the suspension system at 30cm and 36 heights, respectively.

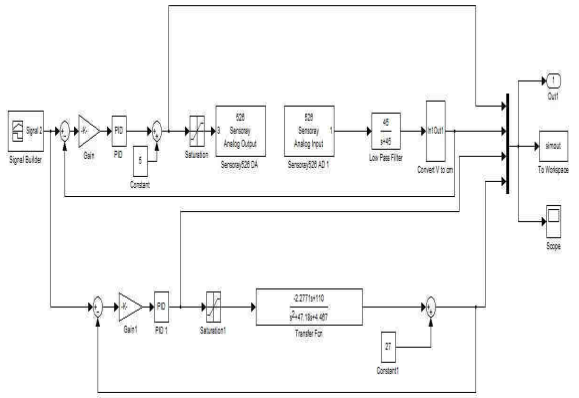

Figure 2 Simulink block diagram for closed loop compensated system

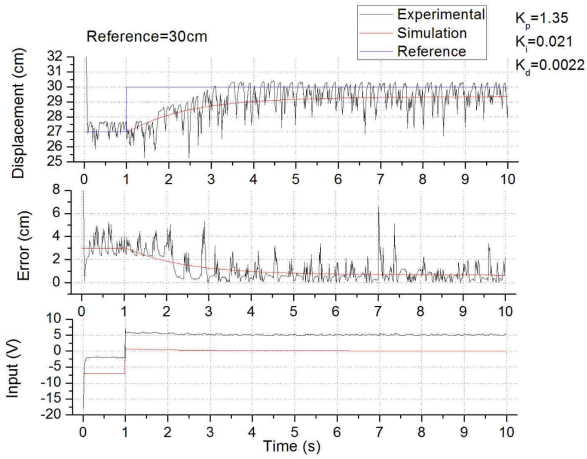

Figure 3 PID compensated system with 30cm reference

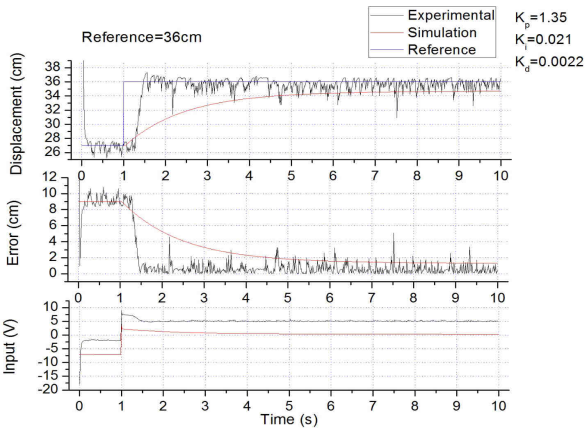

Figure 4 PID compensated system with 36cm reference

Table 1 Transient properties for PID compensated system with 30cm reference

Properties	Experimental	Simulation
Steady-state error (cm)	0.37	0.65
Rise time (s)	1.53	3.31
Overshoot (%)	0	0

Table 2 Transient properties for PID compensated system with 36cm reference

Properties	Experimental	Simulation
Steady-state error (cm)	0.43	1.32
Rise time (s)	0.22	3.21
Overshoot (%)	0	12.02

For reference height 30cm, the PID controller successfully reduced steady-state error from 0.72cm to 0.37cm for the experimental value. The rise time was reduced to 1.53s and 3.31s for the experimental and simulation value respectively, with no overshoot.

4. CONCLUSIONS

As a conclusion, the PID controller with values K_p = 1.35, K_i = 0.021 and K_d = 0.0022 was successfully designed to achieve better system performance. The controller was proven to be able to improve steady-state error by 48.6% and 21.8% for references of 30cm and 36cm respectively, with a slight 12% overshoot for 36cm reference. As for the rise time, the PID controller successfully reduced it by 37.6% and 60% for the 30cm and 36cm, references respectively.

ACKNOWLEDGEMENT

Authors are grateful to Universiti Teknikal Malaysia (UTeM) for supporting the research. This publication is supported by the Fundamental Research Grant Scheme FRGS/1/2016/TK04/FKE-CERIA/F00305.

REFERENCES

[1] S. Prabhakar, and K. Arunachalam, "Simulation and Analysis of Passive Suspension System for Different Road Profiles with Variable Damping and Stiffness Parameters", *Journal of Chemical and Pharmaceutical Sciences,* Special Issue 7, pp. 32-36, 2015.

[2] P. Sharma, N. Saluja, D. Saini, and P. Saini, "Analysis of Automotive Passive Suspension System with MATLAB Program Generation", *International Journal of Advancements in Technology,* vol. 4, no. 2, pp. 115-119, 2013.

[3] P. Krishnasamy, J. Jayaraj, and D. John, "Experimental Investigation on Road Vehicle Active Suspension", *Journal of Mechanical Engineering*, vol. 59, pp. 620-625, 2013.

[4] S.A.A. Bakar, R. Masuda, H. Hashimoto, T. Inaba, H. Jamaluddin, R.A. Rahman, and P.M. Samin, "Ride Comfort Performance of Electric Vehicle Conversion with Active Suspension System", in *SICE Annual Conference 2012*, 2012, pp. 1980-1985.

[5] K. Kamalakannan, A. ElayaPerumal, S. Mangalaramanan, and K. Arunachalam, "Performance Analysis and Behavior Characteristics of CVD (Semi Active) in Quarter Car Model", *Jordan Journal of Mechanical and Industrial Engineering,* vol. 5, no. 3, pp. 261-265, 2011.

Point-to-point positioning and tracking performances of an underactuated robotic hand system

C.K. Yeo, M.M. Ghazaly*, S.H. Chong, I.W. Jamaludin

Center for Robotics and Industrial Automation (CeRIA), Faculty of Electric Engineering, Universiti Teknikal Malaysia Melaka, Hang Tuah Jaya, 76100 Durian Tunggal, Melaka, Malaysia

*Corresponding e-mail: mariam@utem.edu.my

Keywords: Point-to-point positioning, underactuated robotic hand, PD controller

ABSTRACT – This paper presents the Point-to-Point (PTP) positioning and tracking performances for an underactuated Robotic Hand (RH) with PD controller. The introduce of the underactuated robotic hand with wire mechanism is to reduce the complexity of the controller while perform an excellent performance in term of accuracy and time response. The robotic finger is actuated with a DC geared motor connected to a wire and the performance will be analyzed using MATLAB simulink interface with Micro-box 2000/2000C for real time analysis. The control strategy with PD controller had improved the robotic hand performances with error less than 8° and shorter response time of 1s, respectively. However, the PD controller unable to track the signal perfectly as there is error of approximate ±1.5° and the error increase as the frequency increase.

1. INTRODUCTION

Robotic hand is a kind of mechanical hand that had similar functions as human hands which using either an actuator or wire mechanism to obtain the force to provide the motion, action and position. Nowadays, most of the robotic design are depend heavily on the automatic control system to control and monitor the operation of the robots.

An underactuated robotic hand with the use of string is design to reduce the complexity of the robotic hand at the same time can perform an excellent performance. The major characteristic for the term underactuation for current robotic hand research has been determined by the minimization of the amount of input signals of the robotic hand. The underactuation concept is able to reduce the cost development and weight of the robotic hand as previous study [1]. Raymond et al. [2] found that this underactuated robotic hand has the characteristic of highly self- realizing adaptability where the robotic require a controller just for controlling the angle of the actuator and the robotic hand can adapt to the object shape for grasping [3].

Since designing a dexterous and high accuracy of robotic hands is an extremely difficult task, Dollar and Howe [4] stated that the robotic finger which is actuated by a string or wire will function as tendon between joints to contract or relax. The introduction of the wire is to reduce the complexity of the robotic hand with multiple controller [5]. Then, Proportional-Derivative (PD) controller will be used to evaluate the PTP positioning and tracking performance of the actuator due to the simplicity and good performance of the controller.

2. METHODOLOGY

Figure 1 shows the top view of RH system experimental setup. In this research, only one finger will be evaluated which is Finger 5. The robotic hand is control by interfacing with the Micro-box 2000/2000C and MATLAB Simulink. The transfer function of the robotic hand is given by Equation 1. Figure 2 shows the block diagram of the robotic hand.

$$G(s) = \frac{-0.9772s + 829.9}{s^2 + 47.48s + 0.0728} \quad (1)$$

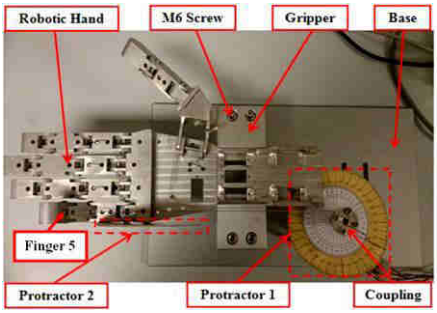

Figure 1 Top View of RH system Setup

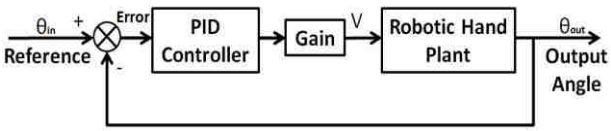

Figure 2 RH block diagram

In this research, two tuning methods are used which are Ziegler-Nichols Second Tuning method with self-oscillation method to obtain the P parameter and trial and error tuning method to obtain the I parameter and D parameter. Ziegler-Nichols Tuning method is the adjustment of the gain until the system start to oscillate with constant oscillation. This constant oscillation occurred is the ultimate gain, Ku with the gain of 483 which is the minimum gain for the robotic hand system that will make the system unstable or marginally stable. Meanwhile the period for the ultimate gain is call as ultimate period, Tu with the period of 0.04s.

PTP positioning control and tracking control are the two experiments that will observe the performance of the designed controller. For PTP control, the reference

position of the robotic finger is changed while for tracking control the type of signal is changed as well as the frequency of the signal.

3. RESULTS AND DISCUSSION

The robotic hand without the controller does not perform well for PTP positioning and tracking control. In this paper, PD controller gain; i.e. K_p=289.8 and K_d=5 are implemented. Figure 3 shows the PTP positioning performance of the robotic hand with PD controller. It can be depicted that the controller able to reduce the error by 8° with an improvement on rise time from 1.213s to 0.213s.

Figure 4 shows the tracking performance of the RH system using sinusoidal signal (0.5Hz) at 30^0 reference. From the graph it can be depicted that the controller unable to track the signal well with error of approximate ±1.5° due to the time response for the PD controller needed to react on the reference signal is too fast.

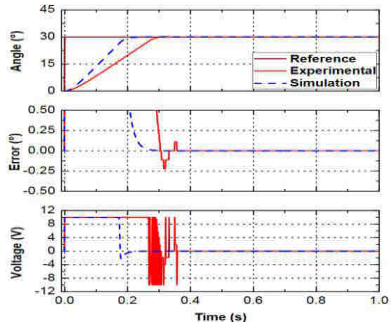

Figure 3 PTP positioning performance of RH, reference at 30°.

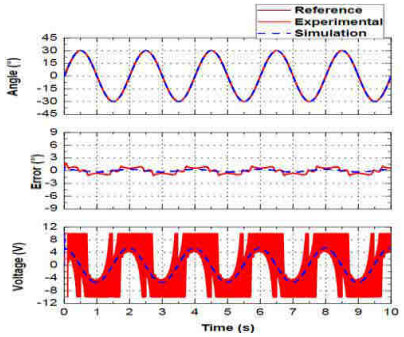

Figure 4 Tracking performance with 0.5Hz sinusoidal reference at 30°

The comparisons between the performance of the robotic hand, with and without the PD controller are shown in the Table 1. The rise time of the robotic hand for 30° has reduce from 1.213s to 0.213s while the steady state error during no controller used is 8.267° was eliminated by using the PD controller. The PD controller also able to eliminate the steady state error in the system for PTP positioning control for 15°, 45°, 60° and 90°. In term of tracking control, the RH does not perform well as error increase when the frequencies increase due to changes of the signal is too fast for PD controller to react. The error for sinusoidal reference 30° occur is approximate ±1.5° but error will increase as frequency increase from 0.5Hz to 2Hz.

Table 1 Comparison of RH performance at 30°

Controller	Rise Time (s)	Error (°)
Without Controller	1.213	8.267
PTP Positioning	0.213	0.000
Tracking Control	-	±1.5

4. CONCLUSIONS

In this paper, the RH was evaluated with the PD controller. The PD controller was introduced to improve the system performances of the robotic hand. The robotic hand was interface with Micro-box 2000/2000C in order to analyze the real time data analysis. The implementation of the PD controller has reduced the rise time for 1s and reduce the steady-state error in the RH system by 8° for positioning control. However, the controller unable to track the reference signals well with error of ±1.5° at frequency of 0.5Hz. For the recommendation, the robotic hand can be further improve by reduce the size of the DC geared motor and a better controller can be designed in order for the robotic hand able to perform well in PTP positioning control and tracking control.

ACKNOWLEDGEMENT

Authors are grateful to Universiti Teknikal Malaysia (UTeM) for supporting the research. This research and its publication are supported by the Fundamental Research Grant Scheme (FRGS) no.FRGS/1/2016/TK04/FKE-CERIA/F00305.

REFERENCES

[1] J. Foody, K. Maxwell, G. Hao and X. Kong, "Development of a Low-Cost Underactuated and Self-adaptive Robotic Hand", in *ASME 2014 International Design and Engineering Technical Conferences & Computers and Information in Engineering Conference*, 2014.

[2] U. O. Lael, R. M. Raymond and M. D. Aaron, "Open-Loop Precision Grasping With Underactuated Hands Inspired by Human Manipulation Strategy," *IEEE Transactions on Automation Science and Engineering*, vol.10, no.3, pp. 625-633, 2013

[3] W. Zhang, L. Tian and K. Liu, "Study on Multi-Finger Under-Actuated Mechanism for TH-2 Robotic Hand", in *Proceeding of the 13th IASTED International Conference Robotics and Application*, 2007, pp. 420-424.

[4] M. Dollar, A., & D.Howe, R., "The Highly Adaptive SDM Hand: Design and Performance Evaluation", *The International Journal of Robotics Research*, vol. 29, no. 5, pp. 585-597, 2010.

[5] M. M. Ghazaly, T. H. Teo, V. Regeev, K. Vijayan, S. H. Chong, A. C. Amran, Z. Abdullah, M. A. M. Ali, "Point-To-Point (PTP) Control Performances of an Upper Limb Robotic Arm", *Jurnal Teknologi*, vol. 78, no. 7,pp 131-140, 2016.